Collisional studies involving N^+ and N_2^+ ions and HgX_2 (X = Cl, Br, and I)

V. Kushawaha, A. Michael, and M. Mahmood
Physics Department, Howard University, Washington, D.C. 20059
(Received 15 January 1988)

Charge transfer reactions involving collisions of N^+ and N_2^+ ions and HgX_2 (X = Cl, Br, and I) molecules have been studied in the kinetic energy range of 1–1000 eV (laboratory frame). Emission spectra from the (B-X) transition of HgX radicals as well as mercury atomic lines from various highly excited energy levels have been observed and analyzed. By using the integrated intensity of the most intense bands of HgX (X = Br or I) radicals and strong mercury atomic lines, emission cross sections have been measured at various laboratory kinetic energies of the projectile ions.

I. INTRODUCTION

Laser action from the (B-X) band system of HgX (X = Cl, Br, or I) radicals has been observed by many investigators in the past[1–18] either by optical or electrical discharge pumping of mercury halide vapors, i.e., HgX_2 (X = Cl, Br, or I) directly or through a mixture of atomic mercury vapors and halogen-containing molecules. The efficiency of these lasers has been observed to increase significantly in the presence of a small amount of neutral gases, such as N_2 and/or Xe,[7–8,11–12] in the discharge medium. This is due to the efficient energy transfer during collisions involving discharge-produced metastables $N_2(A)$ and/or $Xe(^3P)$ and the ground-state HgX_2 vapors leading to the formation of $HgX_2(^{1,3}\Sigma)$. The $HgX_2(^{1,3}\Sigma)$ is a highly repulsive state[19] and dissociates into $HgX(B$ state) and X (X = Cl, Br, or I) atoms. The rate of formation of HgBr(B state) due to collisions of $N_2(A)$ and $HgBr_2$ molecules has been measured by Dreiling and Sester[20] and Chang and Burnham[21] and is equal to 2.8×10^{-11} and 1.0×10^{-10} cm^3 molecule^{-1} sec^{-1}, respectively. No such rate-constant data are available for the B-state formation of HgCl and HgI radicals during the reaction of $N_2(A)$ and HgX_2 (X = Cl and I) molecules. It is to be noted here that the reaction of $N_2(A)$ and $HgCl_2$ leading to the HgCl(B-state) formation is endothermic by about 0.05 eV and no emission has been observed from the B-X transition of HgCl.[20] However, enhanced laser emission has been observed in the presence of N_2 gas in the discharge medium.[7,10] Thus the enhancement of the HgCl laser cannot be explained based on the energy-transfer phenomenon alone. In a discharge medium containing electrons, HgX_2 vapors, and N_2 gas, in the ground and/or electronically excited states, a variety of processes such as excitation, ionization, dissociation, and energy transfer, etc., may take place, leading to the formation of HgX_2^+, HgX^+, Hg^+, N_2^+, and N^+, etc., in addition to $HgX(B$ state) and $N_2(A)$ formation during collisions of electrons and HgX_2 and N_2 molecules. The ionization efficiency of $N_2(A)$ and other highly excited states of N_2 present in the medium, if any, is expected to be much higher than that of the ground-state N_2. Armentrout *et al.*[22] have measured the cross sections for the process $e+N_2(A)\rightarrow N_2^+(X)+2e^-$ in the electron energy range of 11–240 eV with peak cross section of 1.16×10^{-16} cm^2 at 45 eV, whereas Rapp *et al.*[23] have measured the ground-state ionization cross sections of N_2 in the electron energy range of 16–240 eV with peak cross section of 1.9×10^{-16} cm^2 at 100 eV. Recently, Gorman and Zipf[24] have observed the formation of $N_2^+(B$ state) and $N(3P)$ and ground-state N atoms during the collisions of electrons and $N_2(A)$ and have measured the cross sections of these processes, which are more than 0.5×10^{-16} cm^2 at 20 eV. Thus collisions of electrons and $N_2(A)$ in a mercury halide discharge medium may present a serious loss of $N_2(A)$ molecules, leading to the formation of a large number of N_2^+, N^+, and N atoms. However, these ions, i.e., N_2^+ and N^+, when colliding with HgX_2 molecules in the discharge medium, may play a major role in controlling the $HgX(B$-state) formation kinetics at different energies of the projectile ions. Johnsen and Biondi[25] have studied the ion-molecule reactions involving N_2^+ and N^+ with $HgBr_2$ at thermal energy and have observed the formation of $HgBr^+$ and Hg^+ with a rate constant of about 3×10^{-10} cm^3/sec. Such rate measurements have not been reported for $HgCl_2$ and HgI_2 molecules. To the best of our knowledge, chemiluminescent studies involving collisions of these ions at different kinetic energies and ground-state HgX_2 molecules have not been performed and reported in the literature. This information is, however, necessary in theoretical modeling and proper understanding of the discharge kinetics of these lasers.[13,26] In this paper we report our results on the formation of $HgX(B$ state) and highly excited states of atomic mercury during the collisions of N_2^+ or N^+ and HgX_2 vapors at different kinetic energies of these ions. The experimental procedure used and the results obtained will be described below.

II. EXPERIMENTAL PROCEDURE

The charge transfer experiments with N_2^+ or N^+ and HgX_2 molecules were performed by directing mass selected ion beams at a desired kinetic energy into a collision cell containing HgX_2 vapors (Fig. 1). The ions are generated in a low-voltage dc discharge by flowing N_2 gas

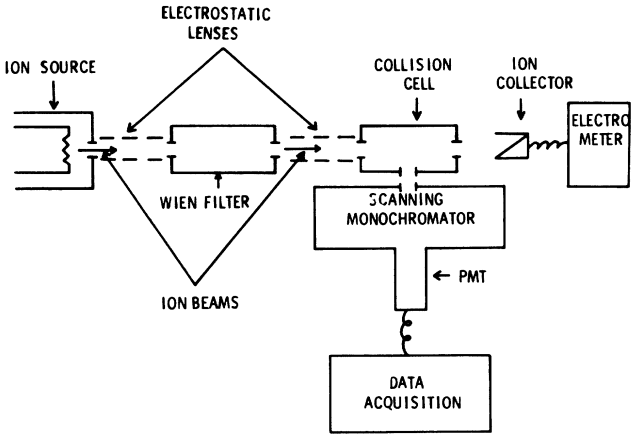

FIG. 1. Experimental setup used in the present study.

through it and extracted from a 0.03-in. hole in the anode and accelerated to an energy of about 1 keV before entering into a high-resolution 6-in. Wien velocity filter.[27] The ions of desired mass at a selected magnetic field pass through the velocity filter undeflected, while ions of different velocities or masses are deflected out of the beam. The desired ions are then decelerated by using a set of electrostatic lenses at different voltages and directed into the reaction cell. These ions are collected on a Faraday cup connected to a high-sensitivity electrometer (Keithley Instruments model 610C) as shown in Fig. 1, to measure the ion currents. The kinetic energy of the reactant ions is adjusted by changing the potential on the collision cell. The electrostatic lenses and the collision cell are made of copper, whereas other focusing elements of the velocity filter are made of high-quality stainless steel. The collision cell has one slot (2 cm×2 mm) parallel to the ion beam and equipped with a sliding suprasil window for monitoring the emitted photons due to the ion/molecule reactions inside the collision cell. This cell also has two apertures for entrance and exit of the ion beam. The mercury halide vapors are generated by heating the desired salts, i.e., $HgCl_2$, $HgBr_2$, or HgI_2, contained in a container located underneath the collision cell. The container is made of copper and wrapped with a band heater capable of raising the temperatures to a maximum of about 450 °C. It is to be noted here that the collision cell and the vapor container are both made of copper and the collision cell is mounted on top of the vapor container, and therefore the temperatures of the vapors and collision cell are assumed to be the same. The temperatures of the mercury halide vapors are measured by a calibrated thermocouple (K-type, Keithley Instruments) and displayed on a digital thermometer. This temperature is then used to calculate the vapor density of all the mercury halides studied here. The Wien velocity filter, collision cell, Faraday cup, and vapor generator are all housed in a stainless-steel chamber which is attached with various view ports. The chamber was evacuated by using two mechanical pumps (Edward model E2M12, 30 CFM) and a cryogenic pump (CTI) model CryoTorr-8) which has a pumping speed of 4000 l/sec for water vapor. With these pumps it was possible to evaluate the chamber to a background pressure of 10^{-7} Torr within a few hours. The pressure was measured by a calibrated Bayer-Lampert ionization gauge. The N_2^+ and N^+ ions were generated by flowing a small amount of N_2 gas into the ion source through a stainless-steel capillary tube, and its flow was controlled by a precision leak valve (Grainville Philiphs model 328).

The light emitted from the collision cell due to reactions of N_2^+ or N^+ ions and HgX_2 (X=Cl, Br, and I) molecules was dispersed by a 0.2-m scanning monochromator equipped with 1200 grooves/mm grating (McPherson model 275 monochromator and model 789 scanner) and detected by a cooled (−25 °C) photomultiplier tube (PMT) (EMI) GenCom model FACT-50 cooler and model 9863QB/5 PMT). The output from the PMT was amplified and displayed on a photon counter (EMI GenCom model Ad-100 amplifier and C-10 photon counter). The signal from the photon counter was either sent to an X-Y chart recorder or to a multichannel analyzer (MCA) (Norland Corp. model 5608). The MCA was interfaced with a digital cassette tape recorder and a plotter for storing and plotting the data. The optical detection system was calibrated by using freshly calibrated deuterium and quartz-halogen lamps (Optronics models UV-40 and 220c) in the wavelength range of 200–800 nm. Various wide bandpass interference filters were used to avoid scattered lights and second-order effect of grating, if any.

The mercury salts, i.e., $HgCl_2$, $HgBr_2$, and HgI_2 were purchased from Alfa Chemical Company with stated purity of 95%. The N_2 gas was supplied by Air-Products with stated purity of 99.9% and was used without further purification.

III. RESULTS AND DISCUSSIONS

During the collisions of N^+ or N_2^+ with HgX_2 (X=Cl, Br, and I) molecules, the emission spectrum of the (B-X) transition of HgX radicals and mercury atomic lines due to radiative transitions from the highly excited states to lower states, i.e., $Hg(7\,^3S_1-6\,^3P_{0,1,2})$ and $Hg(6\,^3D_{1,2,3}-6\,^3P_{0,1,2})$ with the electric dipole selection rule $\Delta J=0,\pm1$, was observed at various laboratory kinetic energies of the projectile ions. In the case of N^+ and $HgBr_2$ collisions, the HgBr (B-X) emission bands were observed to be slightly stronger than those with N_2^+ and $HgBr_2$ collisions, whereas the intensities of the mercury atomic lines were slightly higher with N_2^+ and $HgBr_2$ as compared to N^+ and $HgHgBr_2$ collisions at a particular kinetic energy of the projectile ions, i.e., N^+ or N_2^+. In Fig. 2, we show these results with N^+ and N_2^+ observed at a laboratory kinetic energy of 700 eV and $HgBr_2$ vapor density of about 0.1 Torr. With N^+ or N_2^+ and $HgBr_2$ collisions, these emission bands and mercury atomic lines were observed at laboratory kinetic energy as low as 1 eV. The intensities of these atomic lines and molecular bands were observed to be consistently increasing with increasing kinetic energies of these ions. In Fig. 3 we show these results with N^+ and $HgBr_2$ collisions. The intensity of the HgBr (B-X) bands at low energy with N_2^+ ions was much weaker than those due to N^+ and $HgBr_2$ collisions. This observation indicates that N^+ is more

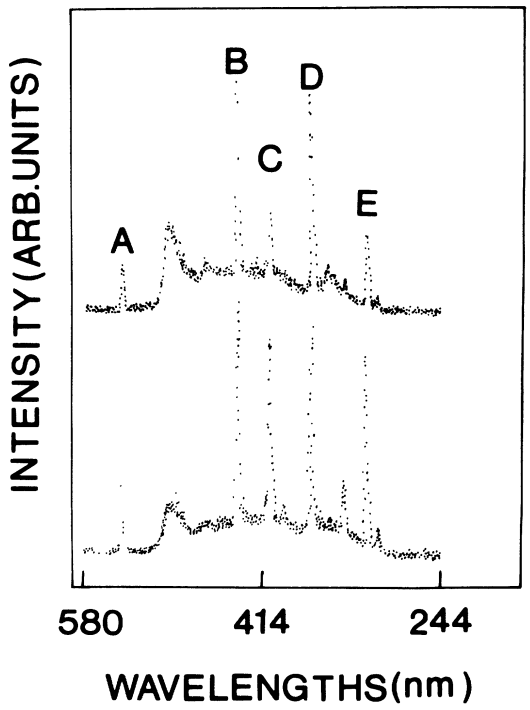

FIG. 2. Emission spectra observed during the collisions of $HgBr_2$ molecules and N^+ and N_2^+ ions at a laboratory kinetic energy of 700 eV. The spectra are uncorrected for the detection efficiency of the optical system. $A=Hg(7\,^3S_1-6\,^3P_2)$, $B=Hg(7\,^3S_1-6\,^3P_1)$, $C=Hg(7\,^3S_1-6\,^3P_0)$, $D=Hg(7\,^3D_3-6\,^3P_2)$, $E=Hg(7\,^3D_2-6\,^3P_1)$. Some of the weaker mercury atomic lines are not labeled.

effective in producing HgBr (B-X) emission than N_2^+. At kinetic energies higher than 200 eV of both of these ions, we observed the mercury emission line at 579 nm, probably due to the (Hg $6\,^1D_2-6\,^1P_1$) transition. The molecular emission bands of the HgBr (B-X) transition were observed to be fully developed in the wavelength range of 520.0–285.0 nm at a higher kinetic energy of the projectile ions, i.e., N^+, or N_2^+ as is generally observed by using the conventional techniques of emission and absorption[28] (see Figs. 2 and 3). Because of the low resolution of our monochromator (4.0 nm/mm dispersion and 20 Å resolution with 500 μm slit width) it was not possible to resolve and identify each bandhead of the B-X transition. However, the most intense bandhead of the HgBr (B-X) transition at 502 nm corresponding to the ($v'=0$)-($v''=22$) transition was clearly visible in all the scans along with intense atomic mercury lines at various kinetic energies of the projectile ions as shown in Figs. 2–4. When $HgBr_2$ was replaced by either $HgCl_2$ or HgI_2 and heated to an appropriate temperature to generate number densities of these species comparable to $HgBr_2$ and the reaction products were observed and analyzed at a particular kinetic energy of the ions, i.e., N_2^+ and N^+, the intensities of the emission bands of the (B-X) transition of HgCl and HgI radicals were observed to be much weaker than those of HgBr. However, the intensities of the mercury atomic lines due to $HgCl_2$ and HgI_2 reactions were observed to be almost identical to those observed due to $HgBr_2$ reactions at an identical kinetic energy of N_2^+ or N^+ ions. In Fig. 4, we display the emission spectrum of the B-X band system of HgX radicals (X=Cl, Br, and I) and atomic lines of mercury due to collisions involving HgX_2 molecules and N^+ ions at a laboratory kinetic energy of 900 eV. The intensity of the B-X bands due to HgCl and HgI radicals was observed to follow the same trend as those of the HgBr radical during the reaction of N^+ and N_2^+, i.e., the emission bands were more intense with N^+ than with N_2^+ at a particular kinetic energy of these ions. However, we were not able to observe any mercury atomic lines or molecular bands with N^+ and $HgCl_2$ collisions at kinetic energies lower than 100 eV. With N_2^+ and $HgCl_2$, on the other hand, we were able to observe atomic lines due to transitions (Hg $7\,^3S_1-6\,^3P_2$) and (Hg $7\,^3S_1-6\,^3P_1$) *only* and no bands down to 1 eV. These observations are inconsistent with the those of N^+ or N_2^+ and $HgBr_2$ collisions. The reasons for this inconsistency are not known to us at this time. In the case of N^+ or N_2^+ and HgI_2 collisions, we

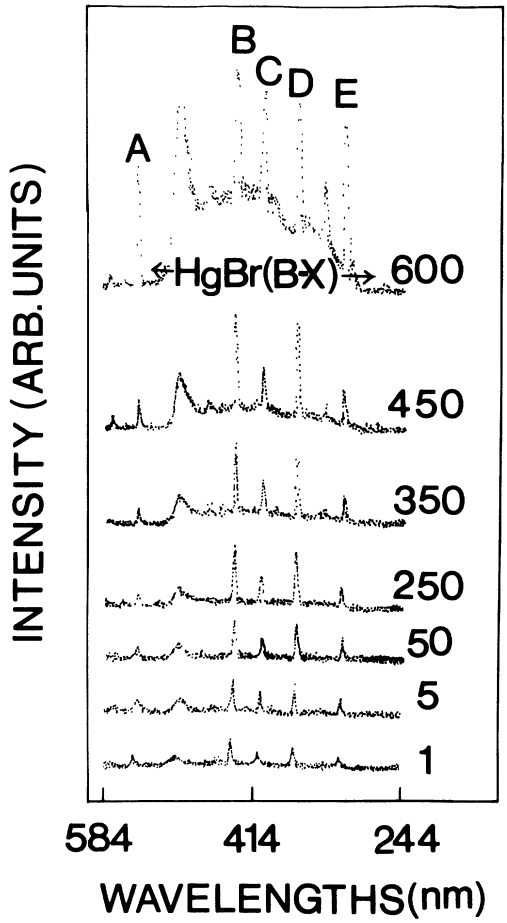

FIG. 3. Variation of intensities of HgBr (B-X) bands and mercury atomic lines observed at various laboratory kinetic enerties (eV) of N^+ during collisions with $HgBr_2$ molecules. The spectra are uncorrected for optical detection efficiency. $A=Hg(7\,^3S_1-6\,^3P_2)$, $B=Hg(7\,^3S_1-6\,^3P_1)$, $C=Hg(7\,^3S_1-6\,^3P_0)$, $D=Hg(7\,^3D_3-6\,^3P_2)$, $E=Hg(7\,^3D_2-6\,^3P_1)$.

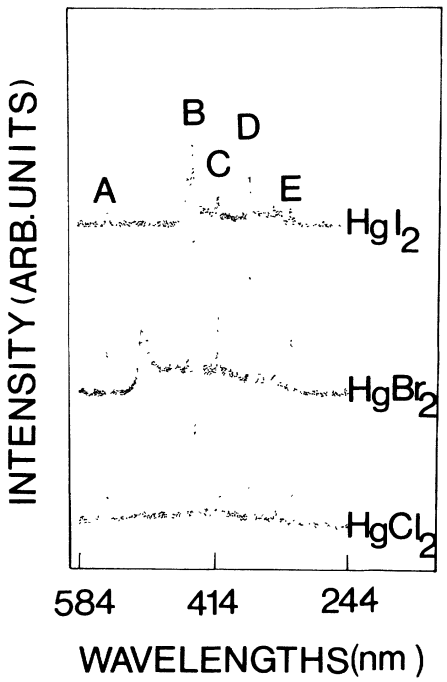

FIG. 4. HgX (B-X) bands and atomic mercury lines observed during collisions of N^+ and HgX_2 (X=Cl, Br, and I) molecules at laboratory kinetic energy of 700 eV. The spectra are uncorrected for optical detection efficiency (see text for details). A=Hg(7^3S_1-6^3P_2), B=Hg(7^3S_1-6^3P_1), C=Hg(7^3S_1-6^3P_0), D=Hg(7^3D_3-6^3P_2), E=Hg(7^3D_2-6^3P_1).

could not observe any atomic lines or molecular bands at kinetic energies lower than 500 eV.

Because of the low vapor density of HgI_2, it was necessary to heat the sample to get a number density comparable to that of $HgCl_2$ or $HgBr_2$ molecules. At higher temperatures, we observed slight coating of either HgI_2 or thermally dissociated I_2 molecules on the viewing window. Under these conditions, the weaker emissions could not be observed even though they were being produced in the reaction cell. We did not, however, observe any such coatings due to $HgCl_2$ or $HgBr_2$ vapors at the temperatures used in the present study.

It is worth noting here that the emission bands and atomic mercury lines shown in Fig. 4 are not corrected for the relative response of the optical system at various wavelengths and therefore it may reflect different intensities than the actual one. However, the absolute response of our detection system at the wavelengths of the most intense bands of the HgX radicals (X=Cl, Br, and I), i.e., 557, 502, and 444 nm, respectively, corresponding to the transition ($v'=0$)-($v''=22$) is not significantly different to affect the peak height of these emission bands or atomic lines. These corrections have been made in calculating the cross sections of the emission bands and mercury atomic lines at various kinetic energies of the projectile ions (see below).

We were unable to observe emission bands of C-X or D-X transition of the HgX radicals in the kinetic energy of range 1–1 keV of the projectile ions N^+ or N_2^+. However, these band systems have been observed in energy-transfer processes, especially from $N_2(A)$ to $HgBr_2$ molecules.[21] The B-X band system of the diatomic halogens, which are observed easily in emission or absorption[28] through the individual vapors and lie in the same wavelength range as used in the present study to observe the emission spectrum of the HgX radicals, were not observed by us. This simply means that either these bands are too weak to be observed with our detection system or these diatomic molecules are not formed during the charge transfer processes studied here. It is also to be noted here that the most frequently observed[29] emissions from the N_2^+ (B-X) transition in a charge transfer reaction involving N_2^+ ions and a variety of target species with the most intense band at 391.5 nm was also not observed in the present studies. However, this and other bands of the N_2^+ (B-X) transition were observed with our detection system during collisions involving N_2^+ and He or He_2^+ and N_2 gas as target at different kinetic energies of the projectile ions. This observation clearly indicates that our detection system is capable of detecting these emissions, if present. Based on these observations and those of Johnsen and Biondi,[25] the following set of reactions may be responsible for the observation of the emission bands of the B-X transition of HgX radicals (X=Cl, Br, and I) and the mercury atomic lines in the present studies and various ions by Johnsen and Biondi.[25]

(a) Direct or collision-induced dissociative charge transfer processes,

$$N^+(N_2^+)+HgX_2 \rightarrow HgX_2^+ + N(N_2)+\Delta E\ , \quad (1)$$

$$N^+(N_2^+)+HgX_2 \rightarrow HgX^+ + X + N(N_2)+\Delta E\ , \quad (2)$$

$$N^+(N_2^+)+HgX_2 \rightarrow Hg^+ + X_2 + N(N_2)+\Delta E\ , \quad (3)$$

$$N^+(N_2^+)+HgX_2 \rightarrow HgX + X^+ + N(N_2)+\Delta E\ , \quad (4)$$

$$N^+(N_2^+)+HgX_2 \rightarrow Hg + X_2^+ + N(N_2)+\Delta E\ . \quad (5)$$

(b) Collision-induced dissociative excitation processes,

$$N^+(N_2^+)+HgX_2 \rightarrow HgX_2^*(^{1,3}\Sigma)+N^+(N_2^+)+\Delta E\ , \quad (6)$$

$$N^+(N_2^+)+HgX_2 \rightarrow HgX^*(B)+X+N^+(N_2^+)+\Delta E\ , \quad (7)$$

$$N^+(N_2^+)+HgX_2 \rightarrow Hg^* + X_2 + N^+(N_2^+)+\Delta E\ , \quad (8)$$

$$N^+(N_2^+)+HgX(X) \rightarrow HgX^*(B)+N^+(N_2^+)+\Delta E\ , \quad (9)$$

$$N^+(N_2^+)+Hg \rightarrow Hg^* + N^+(N_2^+)+\Delta E\ , \quad (10)$$

$$N^+(N_2^+)+Hg^* \rightarrow Hg^{**} + N^+(N_2^+)+\Delta E\ . \quad (11)$$

(c) Radiative decay processes,

$$HgX_2^*(^{1,3}\Sigma) \rightarrow HgX^*(B)+X\ , \quad (12)$$

$$HgX^*(B) \rightarrow HgX(X,v)+h\nu\ , \quad (13)$$

$$Hg^{**} \rightarrow Hg^* + h\nu\ , \quad (14)$$

$$Hg^* \rightarrow Hg + h\nu\ , \quad (15)$$

where HgX_2^+, HgX^+, Hg^+, X_2^+ and X^+ are the ground-state ionized species; $HgX_2^*(^{1,3}\Sigma)$, $HgX^*(B)$, Hg^{**} (i.e., $7\,^3S_1$ states), and Hg^* (i.e., $6\,^3P$ states) are the electronically-excited-state species, $HgX(X,v)$ and Hg are the ground-state species; and ΔE is the exothermicity or endothermicity of the reaction. It is known that the ground-state ionization potentials[30,31] of N and N_2 are 14.54 and 15.58 eV, respectively. The ground-state ionization potentials[31–33] of the mercury halides, i.e., HgX_2, are 11.5, 10.88, and 10.19 eV, whereas those of HgX (Refs. 31 and 32) are 12.06, 11.83, and 10.88 eV, respectively, with X=Cl, Br, and I. For the Hg atom[30] it is equal to 10.44 eV and, for X_2 and X, these values[30,31] are 11.5, 10.52, and 9.31 and 12.96, 11.84, and 10.44 eV for X=Cl, Br, and I, respectively. The ground-state dissociation energies[34,35] leading to $HgX_2 \rightarrow HgX$ are 3.5, 3.12, 2.62, and that[36] of $HgX_2 \rightarrow Hg + X_2$ are 2.52, 1.86, and 1.15 eV (X=Cl, Br, and I), respectively. By using this information on the ionization potentials and dissociation energies of the various species, ΔE for the processes (1)–(5) was calculated and found to be highly exothermic ranging from 0.53 to 5.39 eV (Table I). These values of ΔE indicate that a large number of ions such as HgX_2^+, HgX^+, Hg^+, X_2^+, and X^+ are expected to be produced during the reactions involving N^+ or N_2^+ and HgX_2 molecules. Johnsen and Biondi[25] have, in fact, observed $HgBr_2^+$, $HgBr^+$, and Hg^+ with $HgBr^+$ and Hg^+ being the dominant species, but no indications of Br_2^+ and Br^+ formation are given during collisions involving N_2^+ and $HgBr_2$. These reactions were not studied with $HgCl_2$ and HgI_2 molecules and N^+ or N_2^+ ions. However, the ionic end products of these reactions are expected to be identical to those observed during N_2^+ and $HgBr_2$ collisions, i.e., HgX_2^+, HgX^+, and Hg^+ with no formation of X_2^+ or X^+ ions (X=Cl and I). In the absence of X_2^+ and X^+ ions, the processes (4) and (5) may be ignored. To explain the emission spectrum observed due to the HgX (B-X) and highly excited states of atomic mercury transitions, a process analogous to the collision-induced dissociative charge transfer, i.e., collision-induced dissociative excitation process, may be considered. Such processes have been observed by many investigators in the past by using different species.[29,37] By using the ionization potentials and dissociation energy values given above for all the species of our interest here, the ΔE values for the processes (6)–(11) were calculated and it was found out that these processes are highly endothermic ranging from 2.89 to 6.8 eV (see Table I). The observation of the $HgX(B$ state) and atomic mercury lines from the highly excited states then may be due to the conversion of the kinetic energy of the projectile ions into the internal energy of the reactants. Such a conversion of kinetic energy into the internal energy of products has been observed in the past[29,38] in the kinetic energy range of 4–5 eV. The excited state $HgX_2(^{1,3}\Sigma)$ responsible for the formation of the $HgX(B)$ state due to the predissociative process lies[19,39] at 6.8, 6.3, and 5.51 eV, respectively, with X=Cl, Br, and I, which seems to be a little too high, and the process (6) may not be responsible for the observation of the emission bands from the B-X transition of HgX radicals and the mercury atomic lines from highly excited states. Because of the low dissociation energies of the ground-state species, we believe that the collision-induced dissociative processes such as $HgX_2 \rightarrow HgX(X) + X$ or $Hg + X_2$ or $HgX \rightarrow H + X$ will occur before the excitation processes during the reactions involving N^+ or N_2^+ molecules as indicated above [see reactions (9)–(11)]. These assumptions are supported by the fact that at higher ki-

TABLE I. Exothermicity or endothermicity of the collision-induced processes involving N^+ or N_2^+ and HgX_2 molecules.

Reactions	ΔE X=Cl	Br	I
$N^+ + HgX_2 \rightarrow HgX_2^+ + N$	3.04	3.66	4.35
$N^+ + HgX_2 \rightarrow HgX^+ + X + N$	−1.01	0.41	0.73
$N^+ + HgX_2 \rightarrow Hg^+ + X_2 + N$	1.66	2.26	2.97
$N^+ + HgX_2 \rightarrow HgX + X^+ + N$	−1.91	0.34	1.49
$N^+ + HgX_2 \rightarrow Hg + X_2^+ + N$	0.53	1.19	4.12
$N^+ + HgX_2 \rightarrow HgX_2^*(^{1,3}\Sigma) + N^+$	−6.88	−6.30	−5.57
$N^+ + HgX_2 \rightarrow HgX^*(B) + X + N^+$	−6.42	−6.07	−5.66
$N^+ + HgX_2 \rightarrow Hg^* + X_2 + N^+$	−7.44	−6.78	−6.07
$N^+ + HgX \rightarrow HgX^*(B) + N^+$	−2.89	−2.92	−3.01
$N^+ + HgX \rightarrow Hg^* + X + N^+$	−5.91	−5.62	−5.28
$N_2^+ + HgX_2 \rightarrow HgX_2^+ + N_2$	4.08	4.70	5.39
$N_2^+ + HgX_2 \rightarrow HgX^+ + X + N_2$	0.02	1.44	1.76
$N_2^+ + HgX_2 \rightarrow Hg^+ + X_2 + N_2$	2.67	3.29	4.0
$N_2^+ + HgX_2 \rightarrow HgX + X^+ + N_2$	−0.93	1.38	2.52
$N_2^+ + HgX_2 \rightarrow Hg + X_2^+ + N_2$	1.56	2.22	5.15
$N_2^+ + HgX_2 \rightarrow HgX_2^* + N_2^+$	−6.80	−6.30	−5.57
$N_2^+ + HgX_2 \rightarrow HgX^*(B) + X + N_2^+$	−6.42	−6.07	−5.66
$N_2^+ + HgX_2 \rightarrow Hg^* + X_2 + N_2^+$	−7.44	−6.78	−6.07
$N_2^+ + HgX \rightarrow HgX^*(B) + N_2^+$	−2.89	−2.92	−3.01
$N_2^+ + HgX \rightarrow Hg^* + X + N_2^+$	−5.91	−5.62	−5.28

TABLE II. Measured cross sections of $HgX(B$-state) formation due to N^+ and HgX_2 (X=Br and I) collisions at different laboratory kinetic energies of the projectile ion.

Kinetic energy (eV)	Cross sections (10^{-18} cm^2) X=Br	X=I
1000	0.54	
900	1.34	9.4
700	7.9	6.5
650	8.55	
500	9.87	2.4
450	16.60	
350	19.87	
300	10.87	
250	11.75	
100	6.21	
50	2.71	
25	2.10	
10	1.87	
5	1.87	
1	0.35	

netic energies of these ions, we have observed substantial increase in the atomic and molecular emission intensities (see Figs. 2–4), indicating a large conversion of kinetic energy into the internal energy of the reactants. In fact, at kinetic energies higher than 400 eV, we have observed emission from $Hg(6\,^1D_2-6\,^1P_1)$ at 579.0 nm, which lies at about 1.10 eV above that of $Hg(7\,^3S_1)$, from which emissions have been observed at very low kinetic energies, again indicating an efficient conversion of kinetic energy into internal energy of the products. It is to be noted here that some contribution to the formation of $HgX(B$ state) may come from the chemical reactions involving $Hg(6\,^3P_2)$ and X_2 molecules, if present in the system. The $Hg(6\,^3P_2)$ is a metastable state with the ground state $Hg(6\,^1S_0)$, and emission lines from different transitions such as $Hg(7\,^3S_1-6\,^3P_2)$ and $Hg(6\,^3D_3-6\,^3P_2)$ have

TABLE III. Measured cross sections of $HgX(B$-state) formation due to N_2^+ and HgX_2 (X=Br and I) collisions at different laboratory kinetic energies of the projectile ion.

Kinetic energy (eV)	Cross section (10^{-18} cm^2) X=Br	X=I
900	1.40	1.67
700	4.40	5.38
650	5.60	4.80
500	4.08	1.17
450	3.78	
350	5.90	
300	4.06	
250	3.47	
100	3.20	
50	3.00	
25	2.90	
10	3.10	
5	2.50	
1	2.80	

TABLE IV. Measured cross sections of some of the strongest lines of mercury observed during collisions involving N_2^+ and HgX_2 (X=Cl, Br, and I) at different laboratory kinetic energies of the projectile ion. $A=Hg(7\,^3S_1-6\,^3P_2)$, $B=Hg(7\,^3S_1-6\,^3P_0)$, $C=Hg(7\,^3S_1-6\,^3P_1)$, $D=Hg(6\,^3D_3-6\,^3P_2)$, $E=Hg(6\,^3D_2-6\,^3P_1)$.

Kinetic energy (eV)	Cross sections (10^{-18} cm^2) A			B			C			D			E		
	Cl	Br	I	Cl	Br	I	Cl	Br	I	Cl	Br	I	Cl	Br	I
1000	16.7	24.8		10.8	6.9		3.7	4.7		4.4	3.5		3.0	5.8	
900	11.3	13.8	3.1	8.3	4.6	4	3.2	4.3	5	4.8	2.3	3	4.6	5.5	4
800	10.8			6.9			1.6			2.4			2.5		
700	17.9	13.0	9.0	8.5	4.8	5	2.8	3.3	2	4.4	2.4	3	3.2	4.4	2
650		7.2			2.7			1.5			1.3			2.5	
600	11.6			4.3			1.8			2.1			1.5		
500	14.7	8.8	1.4	4.6	1.9	2	1.5	1.8	1	1.6	1.5	1	1.5	2.0	
450		9.1			1.6			1.1			1.0			2.6	
400	10.5			2.6			1.0			1.3			1.5		
350		6.5			2.4			1.0			1.0			1.9	
300	12.1	5.0		4.5	1.4		2.9	1.6		2.6	0.9		1.7	1.5	
250		4.4			1.2			1.4			0.9			1.7	
200	8.0			1.7			0.8			0.9			0.7		
100	4.0	2.8		0.7	0.7		0.6	1.0		0.4	0.7		0.4	0.8	
50	3.0	2.1		0.6	0.4		0.3	0.5		0.3	0.5		0.5	0.8	
25		2.3			0.3			0.4			0.4			0.3	
10		1.4			0.2			0.4			0.3			0.4	
5					0.3			0.5			0.4			0.4	

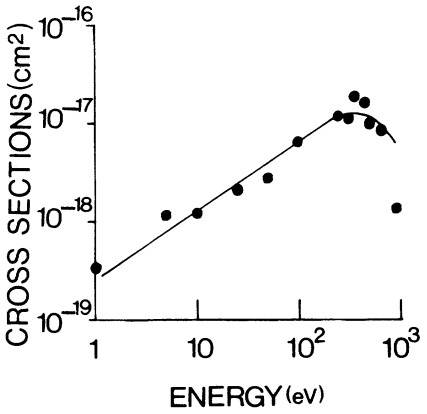

FIG. 5. Measured cross sections of HgX(B state) formation due to N^+ and $HgBr_2$ collisions at various laboratory kinetic energies of the projectile ion. $T(HgBr_2)=110\,°C$.

been observed at various kinetic energies of N^+ and N_2^+ in collisions with HgX_2 molecules generating a pool of these atoms. The $Hg(6\,^3P_2)$ atoms, when colliding with X_2 molecules present in the system may produce a substantial amount of HgX(B-state) radicals. The rate constants for these reactions have been measured[40] to be in the range of 3 to 5×10^{-10} cm^3 molecule^{-1} sec^{-1}.

By using the integrated intensities of the emission bands and atomic lines, an attempt was made to calculate the cross sections of the formation of the excited-state species at different kinetic energies of the ions, i.e., N^+ and N_2^+. These cross sections were calculated by using the expression[41]

$$\sigma = I_s/(I_p n L)\,, \tag{16}$$

where σ is the cross section in cm^2, I_s is the number of emitted photons per second, I_p is the number of charged particles per second, n is the number density of the target species, i.e., HgX_2 (X=Cl, Br, and I) at a particular temperature, and L is the interaction length of the ion beam and mercury halide vapors inside the collision cell. It is

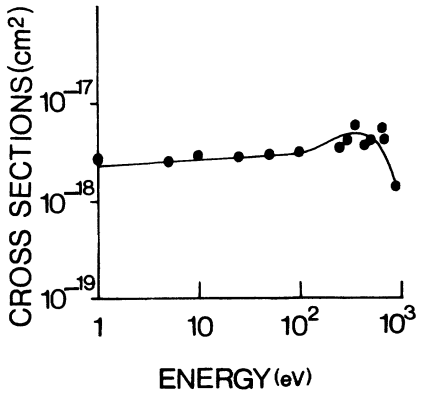

FIG. 6. Measured cross sections of HgX(B state) formation due to N_2^+ and $HgBr_2$ collisions at different laboratory kinetic energies of the projectile ion. $T(HgBr_2)=110\,°C$.

TABLE V. Measured cross sections of some of the strongest mercury atomic lines observed during the collisions of N_2^+ and HgX_2 (X=Cl, Br, and I) molecules at different laboratory kinetic energies of the projectile ion. Note that the cross sections have been rounded off to the first decimal point mainly because of space limitations. In the graph, however, actual numbers have been plotted. The notations A, B, C, D, and E have the same meanings as in Table IV.

Kinetic energy (eV)	Cross section (10^{-18} cm^2)															
	A			B			C			D			E			
	Cl	Br	I	Cl	Br	I	Cl	Br	I	Cl	Br	I	Cl	Br	I	
1000	4.3			1.9			0.8			0.9			0.7			
900	3.9	1.5	2	1.3	0.6	1	0.6	0.3	2	0.7	0.3	2	0.5	0.2	1	
800	5.3			1.9			1.2			1.1			0.9			
700	2.3	7.6	8	1.0	3.6	5	0.5	1.5	3	0.5	1.9	2	0.5	1.5	3	
650		8.1			2.9			1.9			1.6			2.1		
500	1.4	8.0	7	0.5	3.9	2	0.2	1.7	1	0.2	2.1	1	0.2	1.9	1	
450	2	15.4		0.6	6.4		0.3	2.6		0.2	3.3		0.3	2.6		
350		19.0			4.5			3.5			2.2			3.9		
300	0.7	11.6		0.2	4.3		0.1	1.9		0.1	2.1		0.1	2.3		
250	0.6	14.7		0.3	4.9		0.2	2.3		0.1	2.7		0.1	2.5		
100	0.4	5.0		0.1	1.5		0.1	0.7		0.01	0.7		0.01	1.3		
50		2.9			0.9			0.4			0.5			0.6		
25		2.8			0.9			0.3			0.4			0.5		
10		2.5			0.6			0.3			0.3			0.4		
5		1.9			0.6			0.3			0.3			0.4		
1		1.1			0.3			0.3			0.2			0.4		

to be noted here that I_s is the number of photons per second corrected for the optical efficiency of the detection system including the solid angle of light collection subtended by the slit. Because of the weak emissions from the B-X band system of the HgX radicals at low kinetic energies of the projectile ions, we have measured cross sections of the strongest band of this system, i.e., [B, ($v'=0$) to X, ($v''=22$) transition] and only in the case of HgBr and HgI radicals; the emissions from the HgCl(B-X) transition were too weak to be used to measure cross sections and were ignored. In the case of mercury atomic lines we have measured cross sections of only the intense lines due to transitions such as $Hg(7\,^3S_1-6\,^3P_{0,1,2})$ and $Hg(6\,^3D_2-6\,^3P_2)$ with $\Delta J=0$, ± 1. It is also to be noted here that there is no experimental data available on the vapor densities of HgX_2 at various temperatures and therefore we have used the densities of these vapors calculated from the thermochemical data reported by Kubaschewski and Alcock[42] in Eq. (16) to calculate the cross sections. By substituting the appropriate values of I_s, I_p, n, and L in Eq. (16), the cross sections of the emission bands and mercury atomic lines, as discussed above, were calculated at different kinetic energies of N^+ and N_2^+ separately. These results are given in Tables II–V and plotted in Figs. 5–10. Because of the problems associated with the coatings of the HgI_2 vapor on the viewing window, we have measured emission cross sections of HgI(B-X, 0–22) band and atomic mercury lines only at a few kinetic energies of the projectile ions and listed them in the appropriate Tables II–V. These cross sections have not been plotted, however. The accuracy of these cross sections depends upon two fac-

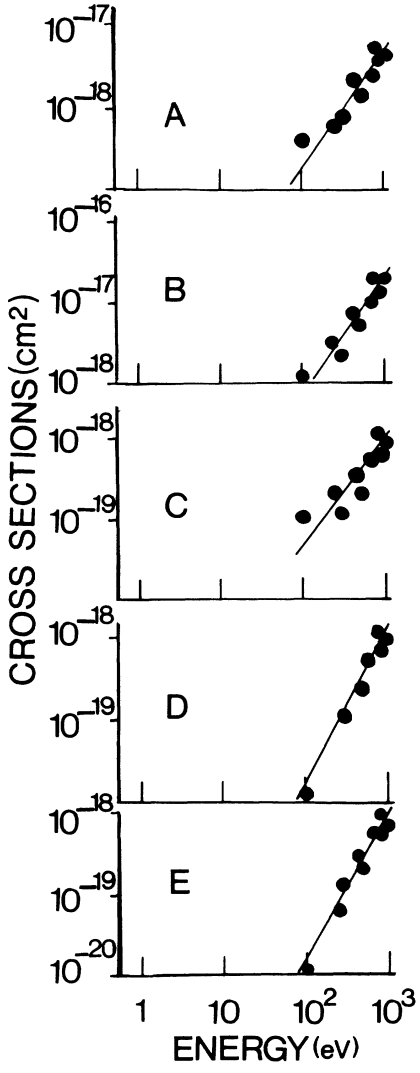

FIG. 7. Measured cross sections of mercury-atomic-lines formation due to collisions of N^+ and $HgCl_2$ at various laboratory kinetic energies of the projectile ion. T ($HgCl_2$)=110°C. $A=Hg(7\,^3S_1-6\,^3P_2)$, $B=Hg(7\,^3S_1-6\,^3P_1)$, $C=Hg(7\,^3S_1-6\,^3P_0)$, $D=Hg(7\,^3D_3-6\,^3P_2)$, $E=Hg(7\,^3D_2-6\,^3P_1)$.

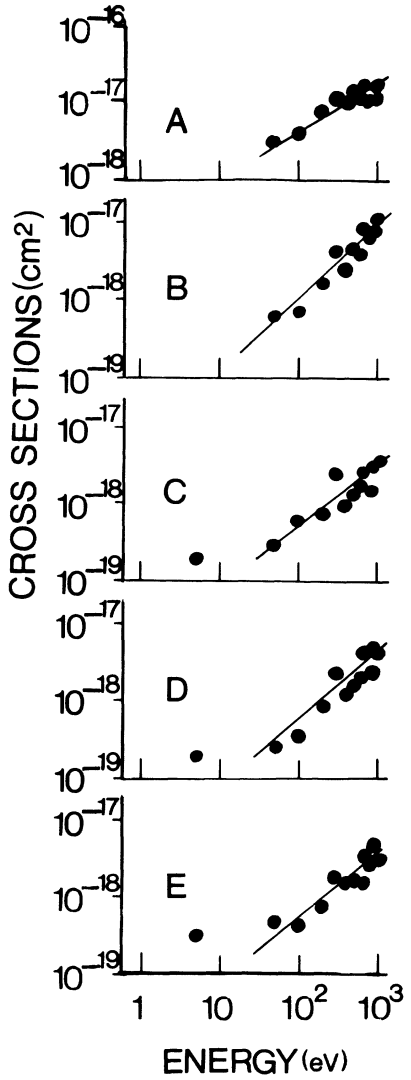

FIG. 8. Measured cross sections of mercury-atomic-lines formation due to N_2^+ and $HgCl_2$ collisions at various laboratory kinetic energies of the projectile ion. T ($HgCl_2$)=110°C. $A=Hg(7\,^3S_1-6\,^3P_2)$, $B=Hg(7\,^3S_1-6\,^3P_1)$, $C=Hg(7\,^3S_1-6\,^3P_0)$, $D=Hg(7\,^3D_3-6\,^3P_2)$, $E=Hg(7\,^3D_2-6\,^3P_1)$.

tors. These are the densities of the vapors and efficiency of detection of the optical system. In the present study, we calibrated our optical detection system using freshly calibrated lamps traceable to the U. S. National Bureau of Standards and rechecked by measuring the emission cross sections of the hydrogen atomic lines observed in charge transfer reactions involving He^+ and H_2 gas at laboratory kinetic energies of 100 and 700 eV. These cross sections were found to be about 20% higher than those measured by Isler and Nathan.[43] Assuming that the calculated vapor densities of the mercury halides, i.e., HgX_2, are fairly accurate, as has been assumed by many investigators in the past,[20,21,39,41] we believe that our measured cross sections should be accurate to within 20–30 %. It is to be noted here that at low kinetic energies of the ions, i.e., below 100 eV, the ion currents were weak and fluctuating and therefore the cross sections at a laboratory kinetic energy of 100 eV or below may be regarded accurate to within 30–50 %.

As indicated earlier in this paper we were unable to observe emission bands of the frequently observed (B-X) band system of the N_2^+ ion during collisions of N_2^+ and HgX_2 (X=Cl, Br, and I) molecules, but if these ions are present in the ground vibrationally excited state, they cannot be monitored by using our present experimental setup. In addition, both N^+ and N_2^+ have metastable states[44] and may contribute to the formation of the excited-state species, but their effect is expected to be insignificant and no consideration has been made in determining the emission cross sections described above.

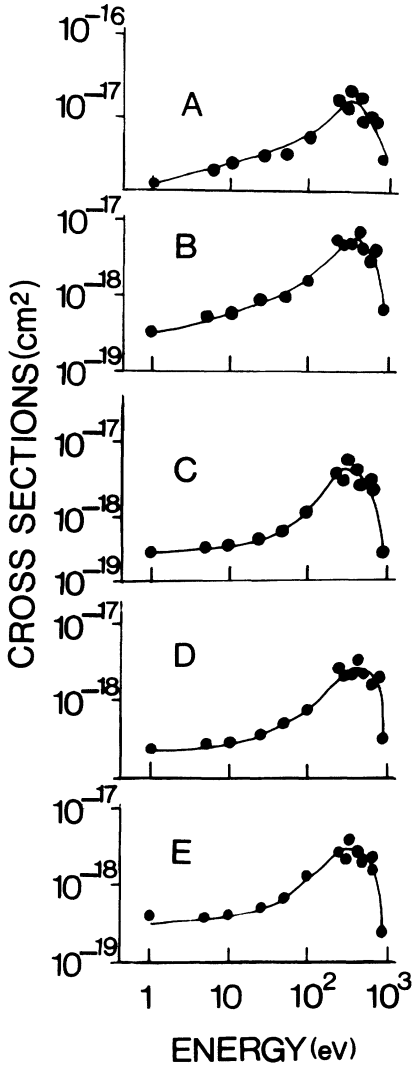

FIG. 9. Measured cross sections of mercury-atomic-lines formation due to N^+ and $HgBr_2$ collisions ar various laboratory kinetic energies of the projectile ion. T ($HgBr_2$)=105 °C. A=Hg($7\,^3S_1$–$6\,^3P_2$), B=Hg($7\,^3S_1$–$6\,^3P_1$), C=Hg($7\,^3S_1$–$6\,^3P_0$), D=Hg($7\,^3D_3$–$6\,^3P_2$), E=Hg($7\,^3D_2$–$6\,^3P_1$).

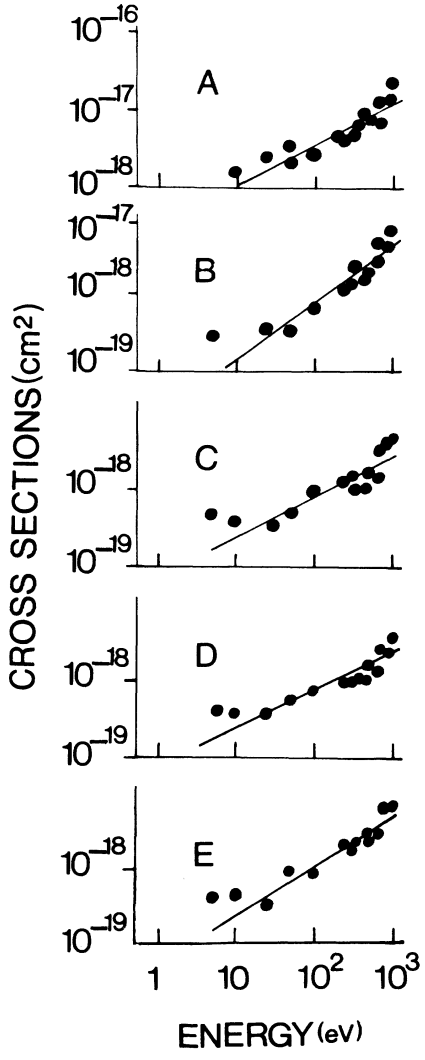

FIG. 10. Measured cross sections of mercury-atomic-lines formation due to N_2^+ and $HgBr_2$ collisions at various laboratory kinetic energies of the projectile ion. T ($HgBr_2$)=105 °C efficiency of the optical system. A=Hg($7\,^3S_1$–$6\,^3P_2$), B=Hg($7\,^3S_1$ –$6\,^3P_1$), C=Hg($7\,^3S_1$–$6\,^3P_0$), D=Hg($7\,^3D_3$ –$6\,^3P_2$), E=Hg($^3D_2$–$6\,^3P_1$).

In conclusion, we have studied the ion-molecule reactions involving N^+ or N_2^+ and HgX_2 vapors at different kinetic energies of the projectile ions. The emission spectrum due to the $HgX(B\text{-}X)$ transition and highly excited states of atomic mercury has been observed and analyzed. By using the integrated intensities of these emissions and calculated values of the vapor densities of HgX_2 molecules, cross sections of the strongest bands of the $B\text{-}X$ transition of HgBr and HgI radicals and atomic lines of mercury have been measured at various kinetic energies of the ions. It has been observed that N^+ ions are more effective in producing $HgX(B\text{-}X)$ emissions than N_2^+ ions. It was possible to observe emissions from $HgBr(B\text{-}X)$ and mercury atomic lines down to 1 eV of the kinetic energy *only* in the case of $HgBr_2$ and N^+ or N_2^+ collisions as compared to N^+ or N_2^+ and $HgCl_2$ or HgI_2 collisions. The collision-induced dissociative processes seem to be the dominant mechanism in producing these emissions.

ACKNOWLEDGMENTS

The research work reported here was supported in part by U. S. Army Research Office Grant Nos. DAAG-29-85-G-0081 and DAAL-03-86-G-010 and by the Research Corporation Grant No. 10938. Partial support was also provided by the Howard University Faculty Research Funds. We are thankful to Bill Pinkney, E. Jones, and George Rambill for help in the laboratory. Thanks are also due to Dr. Lars Wahlin of Colutron Research Corporation for his technical helps in alignments and operation of the mass filter.

[1]J. H. Park, Appl. Phys. Lett. **31**, 192 (1977); **31**, 297 (1977).
[2]J. H. Jacobs, J. A. Mangano, M. Rokni, and B. Srivastava, Bull. Am. Phys. Soc. **23**, 2 (1978).
[3]J. G. Eden, Appl. Phys. Lett. **31**, 488 (1977); **33**, 495 (1978).
[4]J. G. Eden and R. Waynant, Appl. Phys. Lett. **33**, 708 (1978).
[5]W. T. Whitney, Appl. Phys. Lett. **32**, 239 (1978).
[6]E. J. Schimitschek, J. E. Celto, and J. A. Tias, Appl. Phys. Lett. **31**, 608 (1977).
[7]R. Burnham, Appl. Phys. Lett. **33**, 156 (1978); H. J. Baker and N. Seddon, Appl. Phys. B **36**, 171 (1985).
[8]E. J. Schimitschek and J. E. Celto, Appl. Phys. Lett. **36**, 176 (1980).
[9]E. J. Schimitschek and J. E. Celto, Opt. Lett. **2**, 64 (1978).
[10]F. Kvasnik and T. A. King, Appl. Phys. B **32**, 129 (1982).
[11]R. T. Brown and W. L. Nighan, Appl. Phys. Lett. **32**, 730 (1978); **37**, 1057 (1980).
[12]R. Burnham and E. J. Schimitschek, Laser Focus **17**, 54 (1981).
[13]M. W. McGeoch, J. C. Hsia, and D. E. Klimek, J. Chem. Phys. **78**, 1180 (1983); J. Appl. Phys. **54**, 3823 (1983).
[14]T. M. Shay, D. Gookin, M. C. Jordan, F. E. Hanson, and J. E. Schimitsck, IEEE J. Quantum Electron. **QE-21**, 1271 (1985).
[15]T. A. Znotins, C. H. Fishers, T. E. Dehart, J. P. McDaniel, and J. J. Ewing, Appl. Phys. Lett. **46**, 228 (1985).
[16]W. L. Nighan, in *Applied Atomic Collision Physics,* edited by E. McDaniel and W. L. Nighan (Academic, New York, 1982), Vol. 3.
[17]S. P. Bazhulin and N. G. Basov, Kvant. Elektron. (Moscow) **13**, 1022 (1986) [Sov. J. Quantum Electron. **16**, 667 (1986)]; **13**, 1275 (1986) [**16**, 836 (1986)]; **13**, 1386 (1986) [**16**, 908 (1986)].
[18]M. J. Kushner, Mathematical Sciences Northwest, Inc., Report 1984 (unpublished).
[19]W. Wadt, J. Chem. Phys. **72**, 2409 (1980); D. Spence, R. G. Wang, and M. A. Dillon, *ibid.* **82**, 1882 (1985).
[20]T. D. Dreiling and D. W. Sester, Chem. Phys. Lett. **74**, 211 (1980); J. Chem. Phys. **79**, 5439 (1983).
[21]R. S. F. Chang and R. Burnham, Appl. Phys. Lett. **36**, 397 (1980).
[22]P. B. Armentrout, S. M. Tarr, A. Dorri, and R. S. Freund, J. Chem. Phys. **75**, 2786 (1981).
[23]D. Rapp, P. Englander-Golden, and D. D. Briglia, J. Chem. Phys. **42**, 4081 (1965); **43**, 1464 (1965).
[24]M. R. Gorman and E. C. Zipf, in Proceedings of the 34th Gaseous Electronics Conference, Boston, 1981 (unpublished).
[25]R. Johnsen and A. Biondi, J. Chem. Phys. **73**, 5043 (1980).
[26]M. J. Kushner, A. L. Pindroch, C. H. Fisher, T. A. Znotins, and J. J. Ewing, J. Appl. Phys. **57**, 2406 (1985).
[27]Apparatus obtained from Colutron Research Corporation, Boulder, Colorado.
[28]R. W. Pearse and A. G. Gaydon, *Identification of Molecular Spectra* (Chapman and Hall, London, 1963); B. Rosen, *Spectroscopic Data Relative to Diatomic Molecules* (Pergamon, New York, 1970), Vol. 17.
[29]J. D. Kelley, G. H. Bearman, H. H. Harris, and J. J. Leventhal, J. Chem. Phys. **68**, 3345 (1978).
[30]G. Herzberg, *Atomic Spectra and Atomic Structure* (Dover, New York, 1944); R. D. Levin and S. G. Lias, *Ionization Potential and Appearance Potential Measurements,* Natl. Bur. Stand. Ref. Data Ser., Natl. Bur. Stand. (U.S.) Circ. No. 71 (U. S. GPO, Washington, D. C., 1981).
[31]K. P. Huber and G. Herzberg, *Molecular Spectra and Molecular Structure IV. Constants of Diatomic Molecules* (Van Nostrand Reinhold, New York, 1979).
[32]S. H. Linn, J. M. Brom, W. B. Tzeng, and C. Y. Ng, J. Chem. Phys. **78**, 37 (1983); **78**, 50 (1983).
[33]R. W. Kiser, J. G. Dillard, and D. L. Dugger, Adv. Chem. Ser. **72**, 153 (1966).
[34]T. A. Cool, J. A. McGarvey, and A. C. Erlanson, Chem. Phys. Lett. **58**, 108 (1978).
[35]V. I. Vedeneyev, L. V. Gurvich, V. N. Kondratyev, V. A. Medvedev, and Y. L. Frankevich, *Bond Dissociation Energies, Ionization Potentials, and Electron Affinities* (Arnold, London, 1966).
[36]K. Wieland, Z. Phys. **76**, 801 (1932); **77**, 157 (1932); Z. Elektrochem. **64**, 761 (1960).
[37]J. J. Leventhal, in *Gas Phase Ion Chemistry,* edited by Michael T. Bowers (Academic, New York, 1984); Ch. Ottinger, in *ibid.*
[38]G. H. Bearman, S. D. Alspach, and J. J. Leventhal, Phys. Rev. A **18**, 68 (1978).
[39]V. Kushawaha and M. Mahmood, J. Appl. Phys. **62**, 2172 (1987).

[40]T. D. Dreiling and D. W. Sester, J. Chem. Phys. **79**, 5423 (1983), and references therein.

[41]W. L. Nighan, J. J. Hinchen, and W. J. Wiegand, J. Chem. Phys. **77**, 3442 (1982).

[42]The vapor densities of HgX_2 were calculated by using the thermochemical data tabulated by K. Kelley, U. S. Bureau of Mines Reports No. **371**, 1934, and No. 393, 1936 (unpublished); L. Quill, *The Chemistry and Metallurgy of Miscellaneous Materials,* 5th ed. (McGraw-Hill, New York, 1950); O. Kubaschewski and C. B. Alcock, *Metallurgical Themochemistry,* 5th ed. (Pergamon, New York, 1967), p. 54. These values were found to be approximately the same at a particu-densities calculated by using the formula given by Kubaschewski and Alcock.

[43]R. C. Isler and R. D. Nathan, Phys. Rev. A **6**, 1036 (1972).

[44]Ch. Ottinger and J. Simons, Chem. Phys. **28**, 97 (1978).